

Comparisons of VHF Meteor Radar Observations in the
Middle Atmosphere With Multiple Independent Remote
Sensing Techniques.

Daniel L. McIntosh, BSc. (Hons)

Thesis
submitted for the degree of
DOCTOR OF PHILOSOPHY
at the
UNIVERSITY OF ADELAIDE
School of Chemistry and Physics
Discipline of Physics

August 2009

Appendix A

Design Equations for Folded Dipole

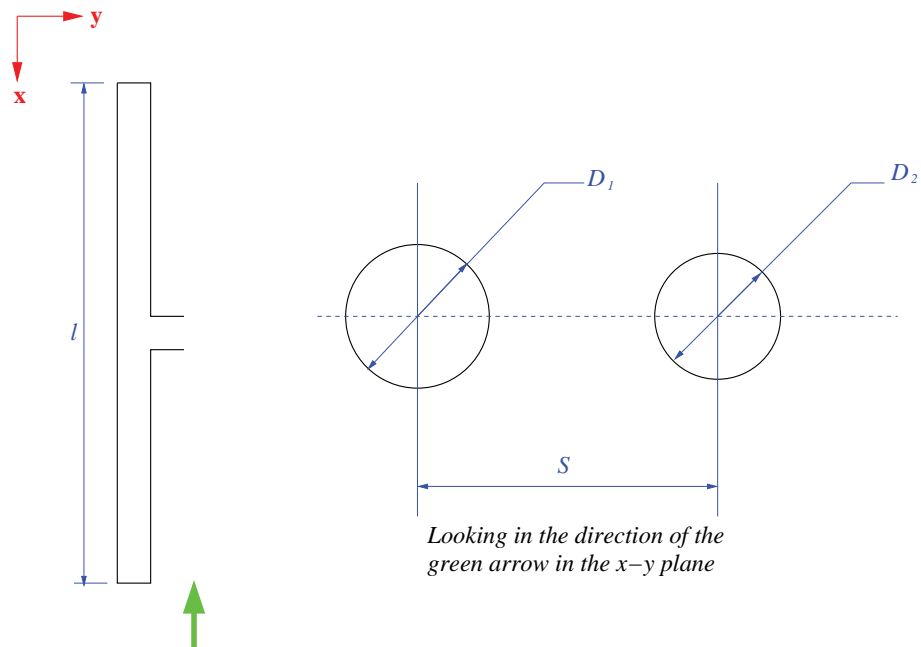


Figure A.1: Folded dipole general dimensions.

The following design formulae are outlined in detail in the paper by Green [1966]. The input admittance formula for a folded dipole is given by:

$$Y = \frac{1}{MZ_D} - \frac{j}{2Z_o \tan(\frac{\beta l}{2})} \quad (\text{A.1})$$

where

- Z_D is defined as the approximate input impedance of the equivalent linear dipole.
- M is the impedance multiplication ratio.
- Z_o is the characteristic impedance formed by the arms of the dipole
- l is the overall length of the dipole.

For $l = \frac{n\lambda}{2}$ then we obtain

$$Y = \frac{1}{MZ_D} \Rightarrow Z = MZ_D \quad (\text{A.2})$$

$$M = (1 + a)^2 \quad (\text{A.3})$$

$$a = \frac{\cosh^{-1}[(4w^2 - v^2 + 1)/4w]}{\cosh^{-1}[(4w^2 - v^2 + 1)/4vw]} \quad (\text{A.4})$$

$$D = D_1 e^{(v^2 \log(v) + 2v \log(2w)/(v^2 + 1))} \quad (\text{A.5})$$

$$v = \frac{D_2}{D_1} \quad (\text{A.6})$$

$$w = \frac{s}{D_1} \quad (\text{A.7})$$

Where

- D_1 is the diameter of the driven arm
- D_2 is the diameter of the non-driven arm
- D is the diameter of the equivalent linear dipole
- S is the conductor centre line spacing
- w is the spacing ratio

Appendix B

Radar Power Calibration Experiment

B.1 Aim

Derive a relationship between the actual transmitted power from the radar and the power setting control of the ATRAD radar configuration software in order to verify the count rate curves as established by McKinley's equation:

$$N \propto \frac{P_t^{1/2} G \lambda^{3/2}}{P_r^{1/2}} \quad (\text{B.1})$$

The method of performing the power calibration measurements on the two different Buckland Park systems (VTX and STX-II) is the same despite the differences in connectivity of the 1:2 and 1:6 splitter-combiners used with the systems.

B.2 Equipment

Required equipment for making the necessary measurements.

1. Signal generator capable of producing a stable frequency at VHF.
2. $3 \times$ “N-type” or equivalent 50Ω dummy loads
3. Vector volt meter or oscilloscope
4. $3 \times$ “7/16” DIN male to female N-type adapter
5. $3 \times$ RG-213 cables with N-type connectors
6. $3 \times$ RG-58 cables with BNC connectors
7. $3 \times$ T-pieces
8. $3 \times$ N-type to BNC adapter

B.3 Making Voltage Measurements on a Power Splitter

When making voltage measurements (as described in the following sections) it is important to realise that the device is in fact a power splitter circuit and not a voltage splitter circuit. This means for the 1:2 splitter-combiner, the voltages do not split in the ratio 1:2. See below.

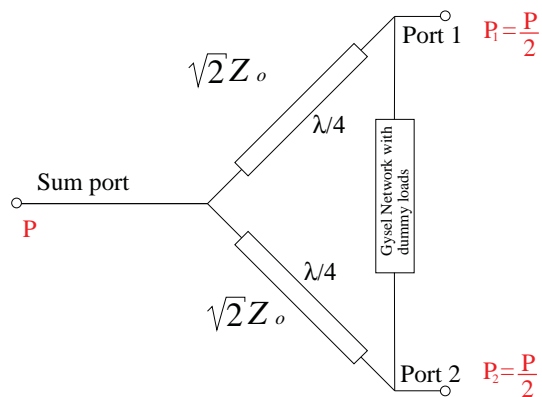


Figure B.1: 1:2 splitter combiner electrical layout diagram.

$$P = \frac{V^2}{Z_0} \quad P_{\text{port}} = P_1 = P_2 = \frac{V_{\text{port}}^2}{Z_0}$$

$$\begin{aligned} P &= P_1 + P_2 = 2P_{\text{port}} \\ \Rightarrow P_{\text{port}} &= \frac{P}{2} \\ \Rightarrow \frac{V_{\text{port}}^2}{Z_0} &= \frac{V^2}{2Z_0} \\ \Rightarrow V_{\text{port}}^2 &= \frac{V^2}{2} \\ \therefore V_{\text{port}} &= \frac{V}{\sqrt{2}} \end{aligned}$$

In general for a N-port splitter-combiner the voltage relation between the sum port and any of the other ports is:

$$V_{\text{port}} = \frac{V_{\text{Sum}}}{\sqrt{N}}$$

It is important to take note of potential sources of loss (attenuation) in making measurements. Some coaxial cable (e.g. RG-58) can exhibit up to 0.5 dB of loss. This amount of loss can lead to as much as a 10% error in the power calculated from voltage measurements. Before undertaking any of the measurements as outlined in the subsequent sections, it is important to quantify the loss introduced by the cables used by using the manufacturer's specification and performing calibration measurements with the cables to be used.

B.4 Measuring Directional Coupler Calibration Factor

It is possible to measure the output power from the radar transmitter by means of measuring the voltage on the forward monitor port of the 1:2 splitter-combiner. The monitor ports are connected to a micro-strip directional coupler which is located along the sum port line on the 1:2 PCB as can be seen in Figure 5.6. The directional coupler has a induced current flow due to the current flowing along the sum-port line thus enabling us to deduce

what the voltage is on the sum-port. In order to make use of these ports we need to determine the associated calibration factor; i.e. just how much of the power flowing through the sum port on the splitter is being sensed by the micro-strip coupler. In the absence of having an appropriate network analyser, we are able to determine this with the equipment listed above. The calibration factor in dB is determined by using the following expression:

$$C = 20 \log_{10} \left(\frac{V_o}{V_i} \right) \quad (\text{B.2})$$

where V_i is the input signal voltage and V_o is the voltage measured on the monitor port.

B.4.1 Determining the Calibration Factor for Monitor Port M1

This will be the forward port when the device is being used as a splitter and the reflected port when used as a combiner.

1. Disconnect the 6:1 combiner from the sum port and connect the signal generator to the sum port using a 7/16 N-type adapter.
2. Disconnect the 2 output/input ports on the 1:2 splitter and terminate the ports with 50Ω dummy loads using the 7/16 DIN Male to female N-type adapter and dummy load or equivalent BNC adapter and BNC 50Ω dummy load .
3. Terminate monitor port M2 on the 1:2 splitter with a N-type dummy load or suitable equivalent.
4. Connect the vector volt meter or oscilloscope to the forward port. When connecting the oscilloscope be sure to use either the 50Ω internal termination on the oscilloscope (if available) or a T-piece with a 50Ω terminator on it.
5. Measure the voltage on port M1 and calculate the calibration factor of the micro-strip coupler using the above equation.

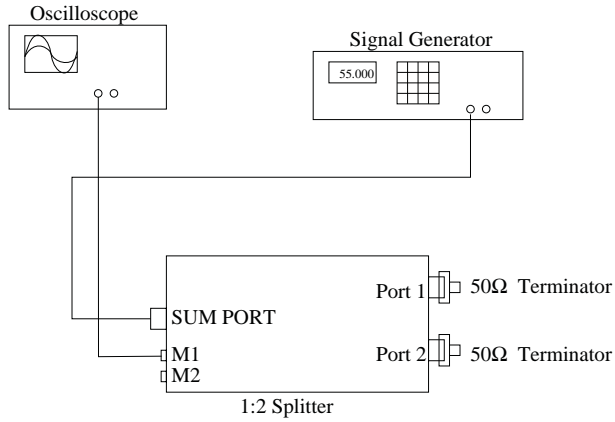


Figure B.2: Setup diagram for measuring monitor port calibration when the splitter combiner is used with a VTX system.

When the 1:2 is used in conjunction with the STX-II system, the flow of current is in the opposite direction and hence we need to determine the calibration factor for port M2. In this case the the test setup can be seen in Figure B.3

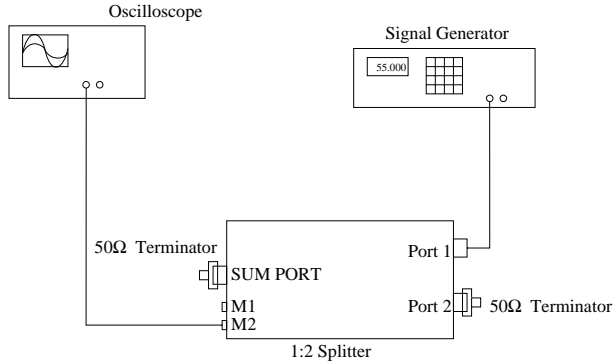


Figure B.3: Setup diagram for measuring monitor port calibration when the splitter is used with a STX-II system.

B.5 Determining the Losses Inside the Splitter and the Balance of the Output Power

In order to measure the loss in the 1:2 splitter, we can measure what the output voltage is from each of the outputs and add them together. We can then calculate the loss in dB using Equation (B.2). For a more accurate approach we can use the Vector Voltmeter which provides both magnitude and phase and then calculate the vector sum of both outputs which can then be compared with the input reference signal.

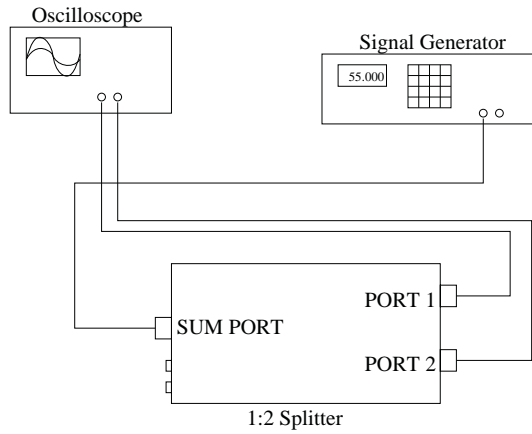


Figure B.4: Setup diagram for measurements.

B.6 ATRAD Software Power Slider Calibration

We want to determine what the physical correspondence between what the software power slider indicates and what physically is transmitted to the antenna. In order to do this we need to reconnect all the components back to the original configuration for normal operation and connect the oscilloscope up to the forward port (M1 for VTX or M2 for STX-II operation) of the 1:2 splitter. See Figure below.

1. Connect all the components up in the appropriate configuration as indicated in Figure B.5 or Figure B.6.
2. Start the radar using the normal experiment parameters
3. Measure the forward voltage on the forward port of the 1:2 splitter with the oscilloscope
4. Once an accurate measurement has been made stop the radar and calculate the power being fed into the splitter using Equation (B.2).
5. Using the radar config software, setup an experimental sequence with a series of experiments with same parameters but different Tx power levels. For example, vary the Tx power percentage by 10% which will give a series of experiments with Tx power levels ranging from 10% to 100% in 10% power level increments.
6. Run the experiment sequence to obtain a baseline for calibration.

B.7 McKinley Count Rate Curve Verification

The final stage involves operating the radar at the same power percentage markers that were used in determining the base-line calibration in the previous section. The experimental sequence is required to be setup with the radar configuration software. the procedure for setting up the experiment is as follows:

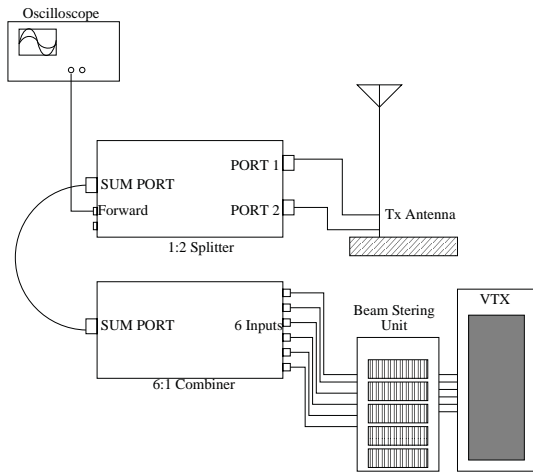


Figure B.5: Setup diagram for VTX system measurements.

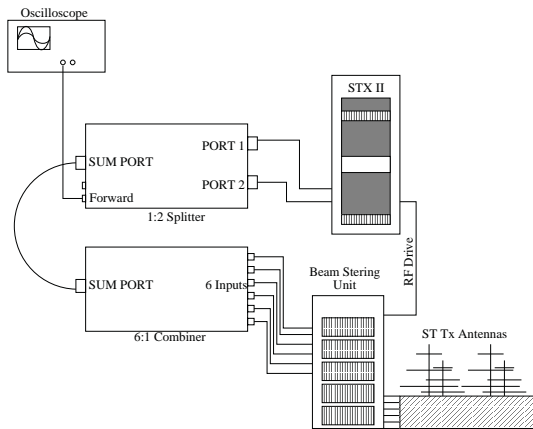


Figure B.6: Setup diagram for STX II-40 system measurements.

1. Determine what percentage power levels to run the experiment at.
2. Using a normal meteor observation experiment for the system in question, use the “Edit As” feature from the the “File” drop down menu. This way all the experimental parameters will be copied over for the new experiment.
3. change the experiment name to *Experiment name XXX* and the experiment tag to *Experiment_tag_XXX* where *XXX* is the percentage power level the radar is being run at. Do this for all the power levels required and then add them to the experimental sequence.

4. Once this is complete, save the experiment sequence changes and then select the experiment sequence containing the experiments from the drop down menu and start the radar.
5. In the ATRAD analysis suite, select “Analysis Control” → “Met” → “Configure”. Set the appropriate analysis channels etc and experiment name and tags.
6. This will produce the required *.met* analysed data file to be used.

The radar is operated over say a 4 day period such that we can obtain a more statistically accurate estimate for the count rates at each power level. The daily count rate for each power level can be estimated by multiplying the number of echoes in each of the daily analysed met files by the weighting factor associated with the experiment. For example, if the radar was run at 25% power levels (i.e. 25%, 50%, 75%, 100%) then you would multiply the counts for each of those analysed files by 4 which would give you the effective daily count rate for running the radar at that power level. The standard deviation of the data can be used as an estimate of the error bars. The results can then be compared with the theoretical results generated with the expression given in Equation (B.1). While the actual received power will not be known with 100% accuracy, an average theoretical value can be used until one can be directly measured.

Appendix C

Supplementary Winds Analysis Results

C.1 Davis Meteor and MF Winds Comparison

The following plots are supplementary results obtained during the course of analysing winds from different locations.

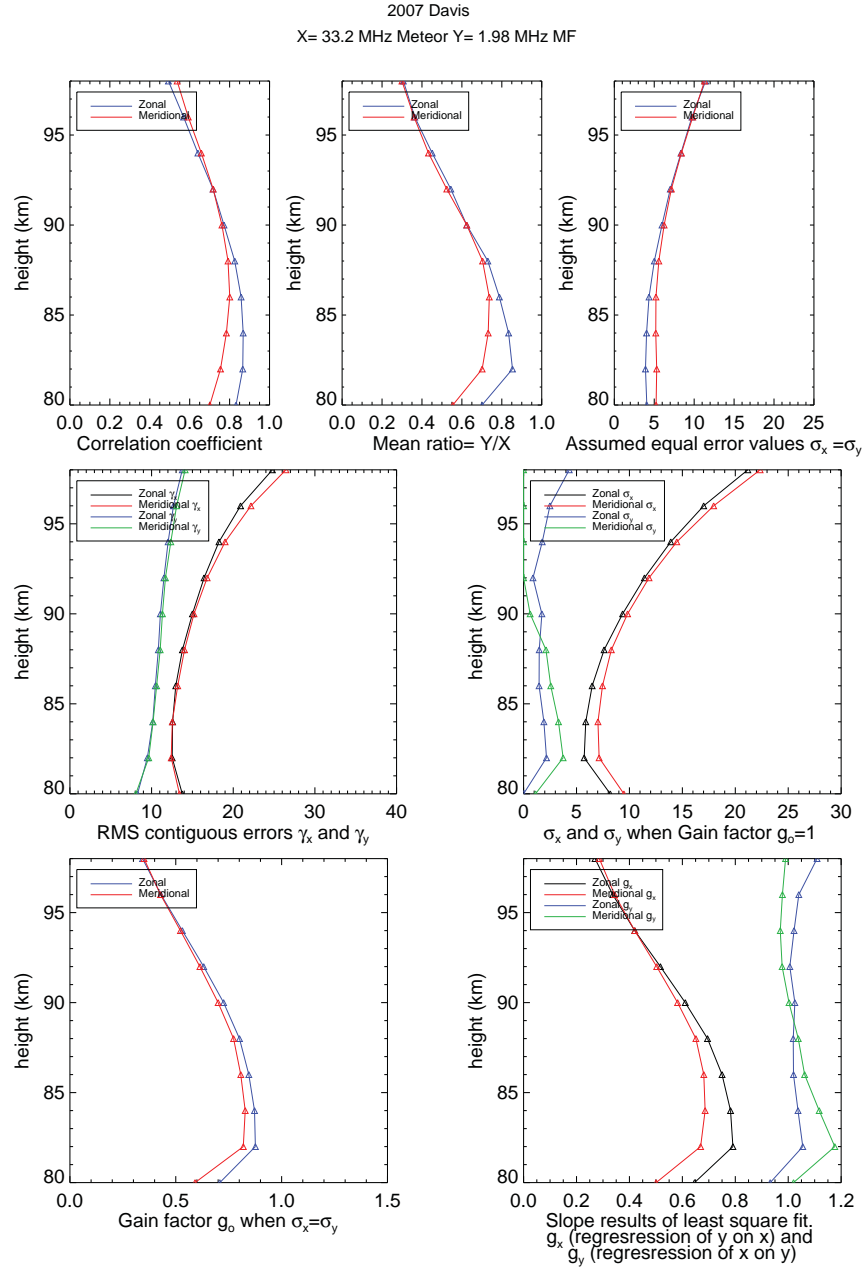


Figure C.1: Davis MF O-mode and 33.2 MHz meteor scatter plot comparison.

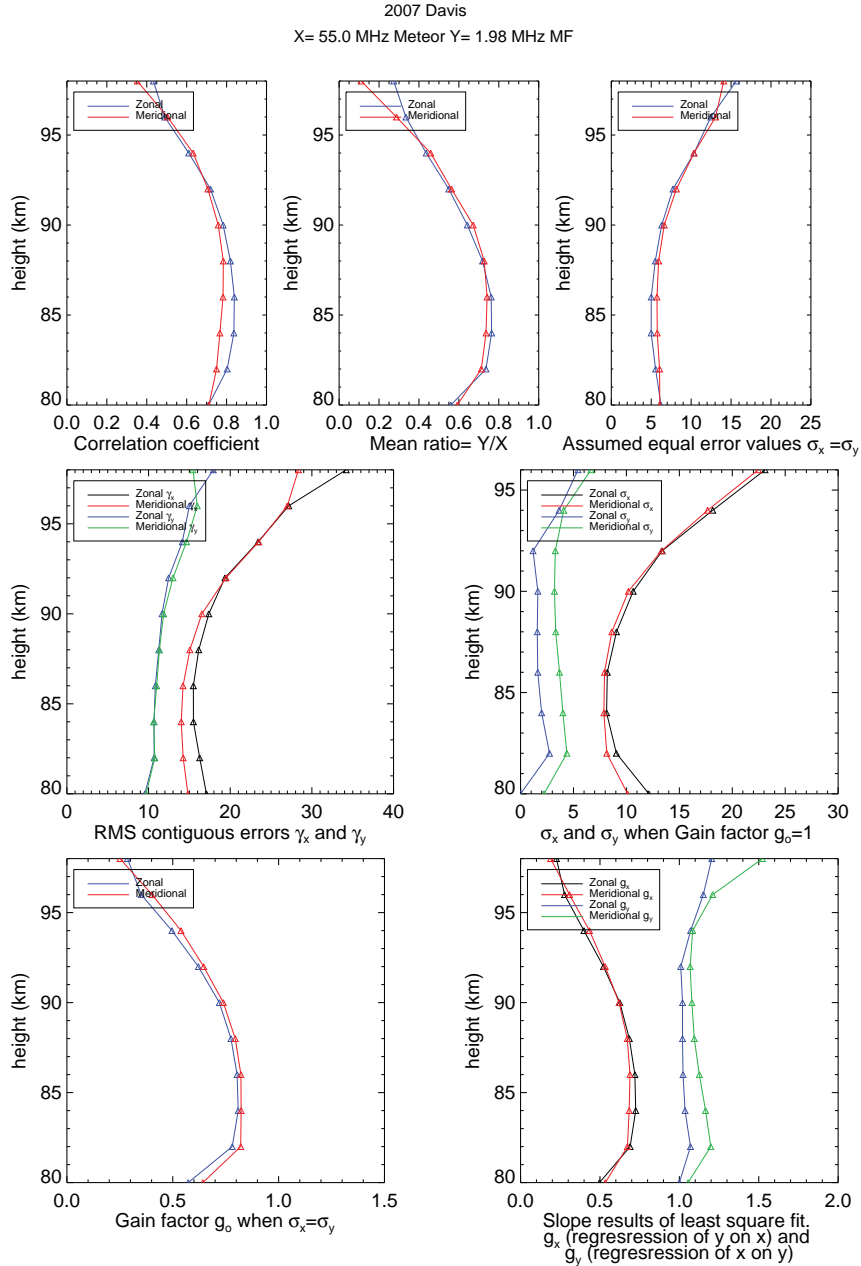


Figure C.2: Davis MF O-mode and 55 MHz meteor scatter plot comparison.

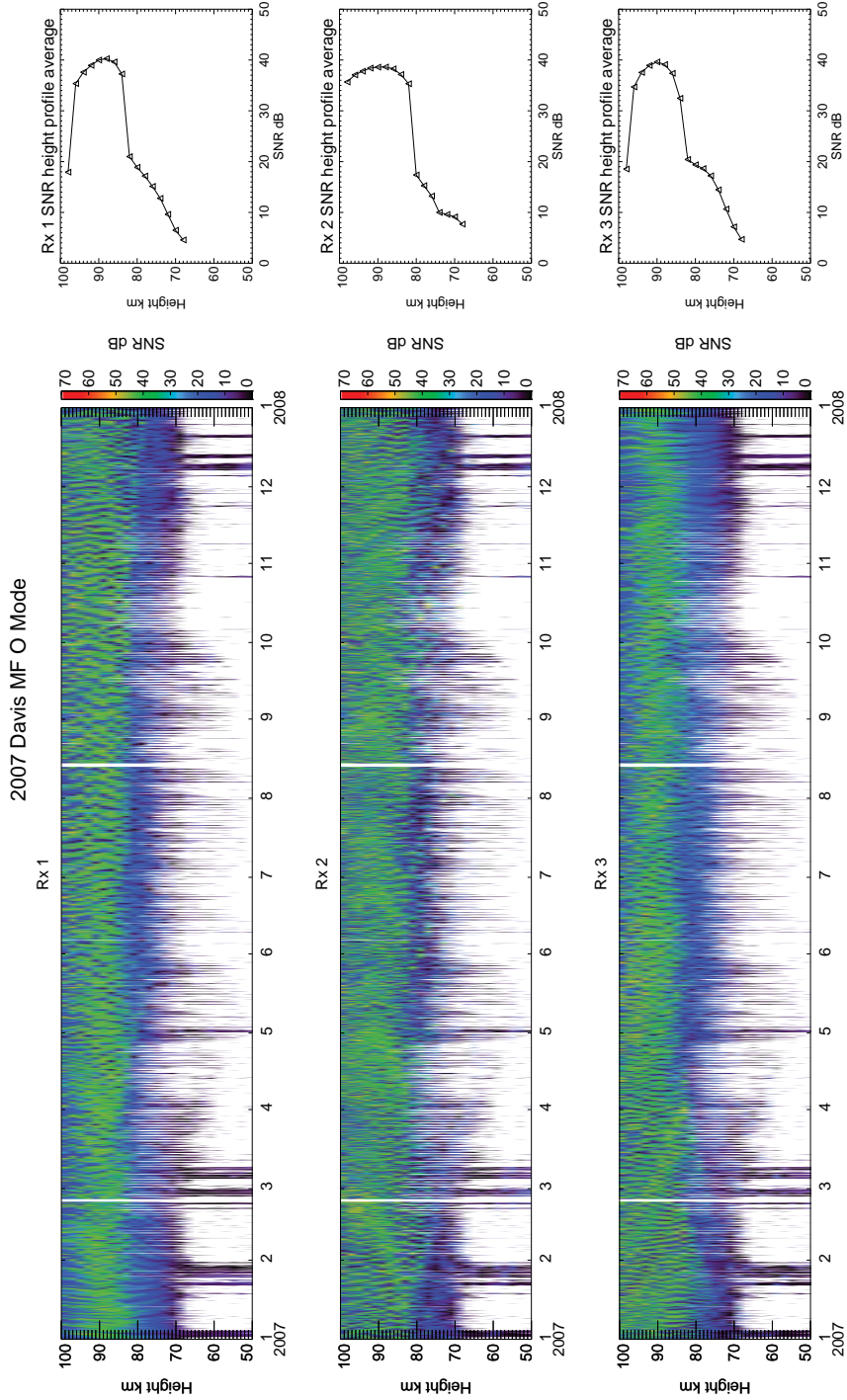


Figure C.3: 2007 Davis MF O-mode SNR.

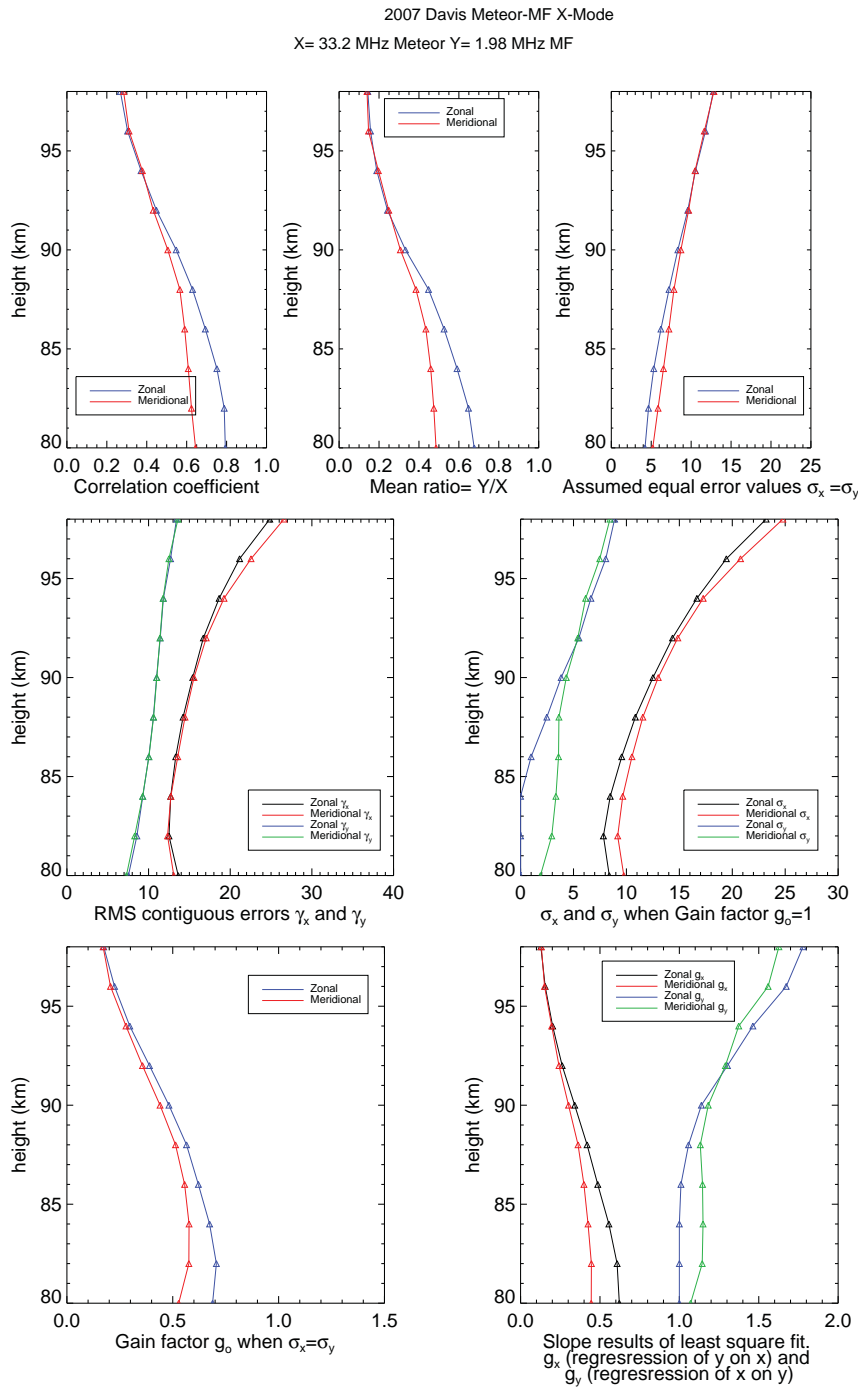


Figure C.4: Davis 33.2 MHz and X mode scatter plot comparison summary.

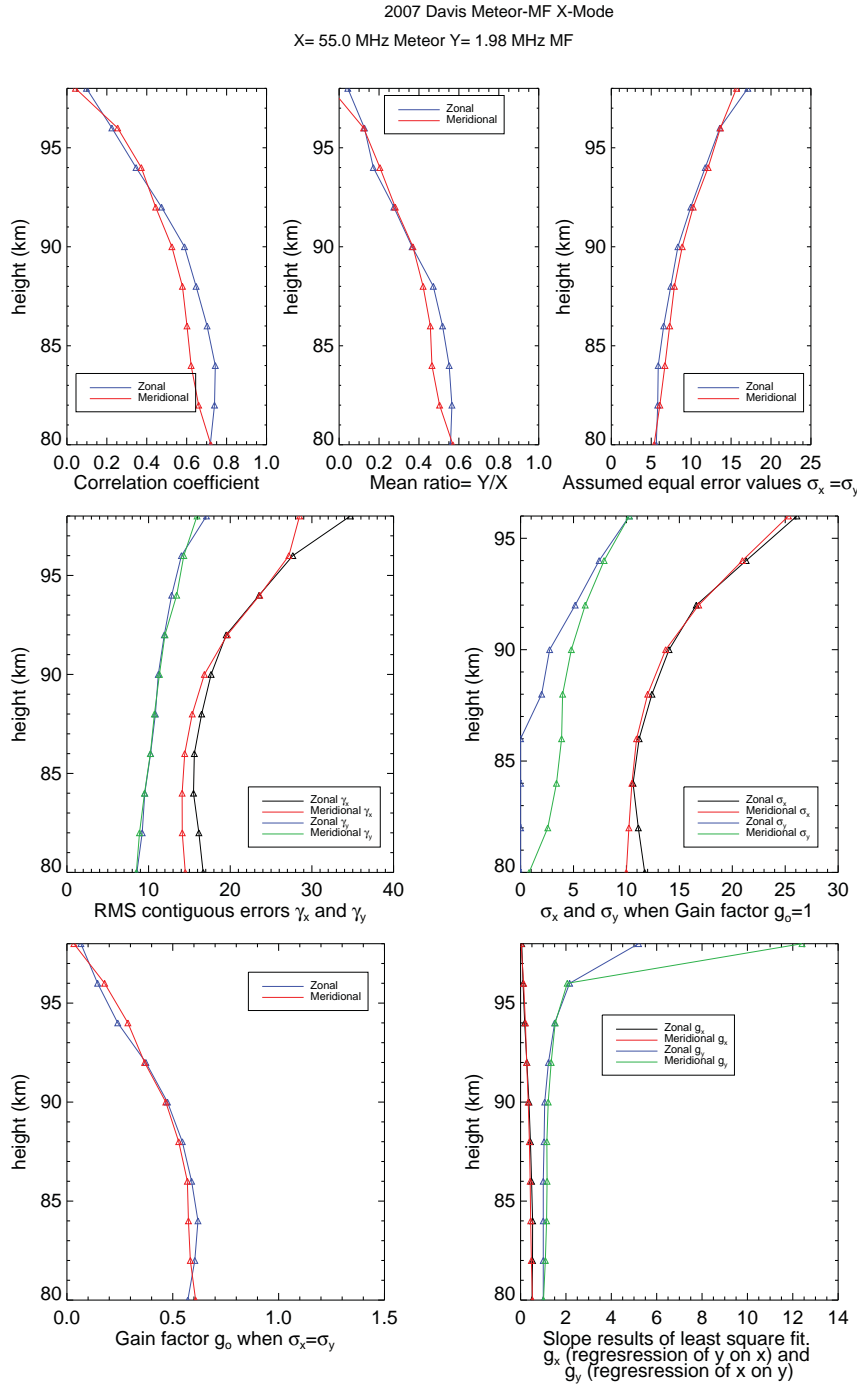


Figure C.5: Davis 55 MHz and X mode scatter plot comparison summary.

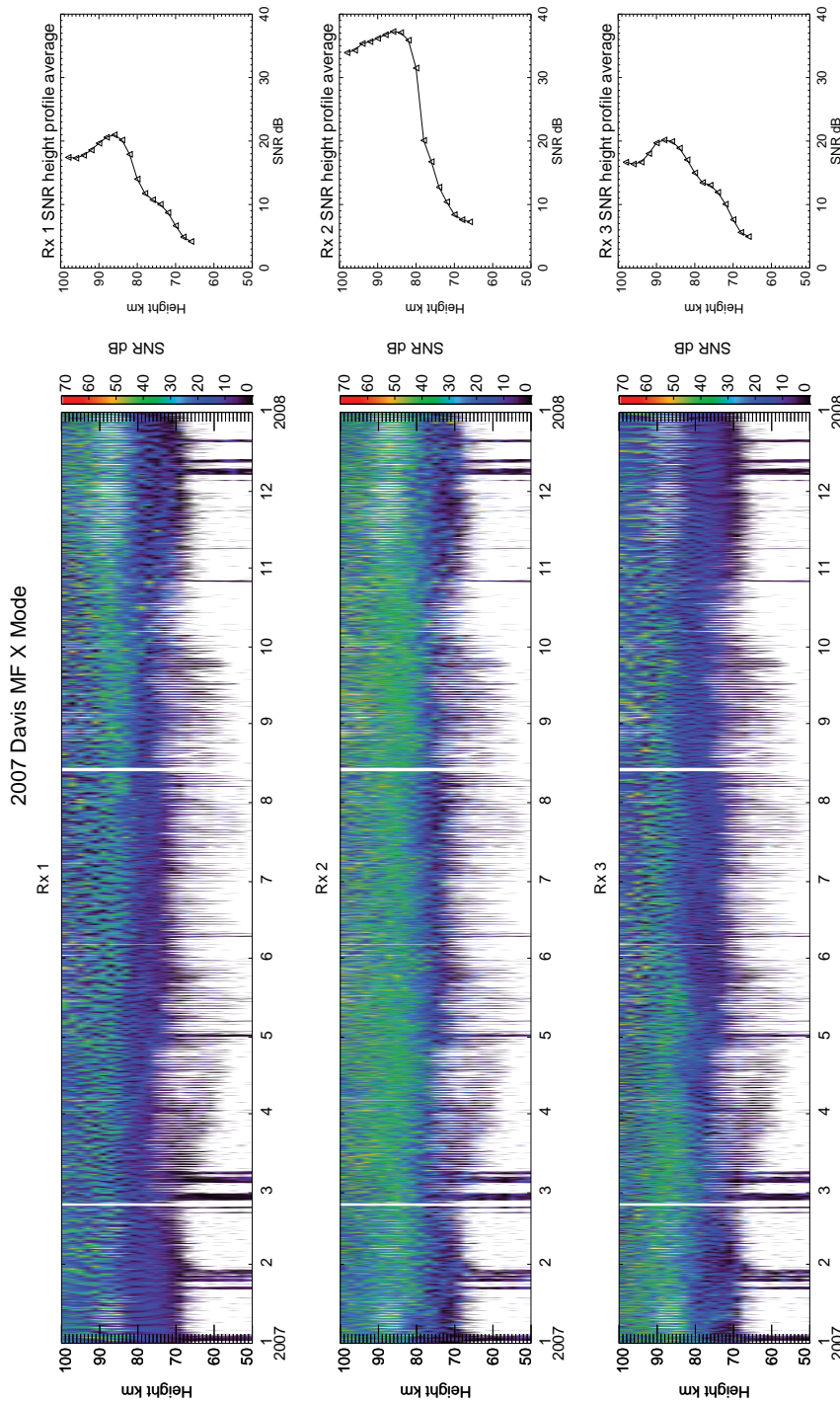


Figure C.6: 2007 Davis MF X mode SNR.

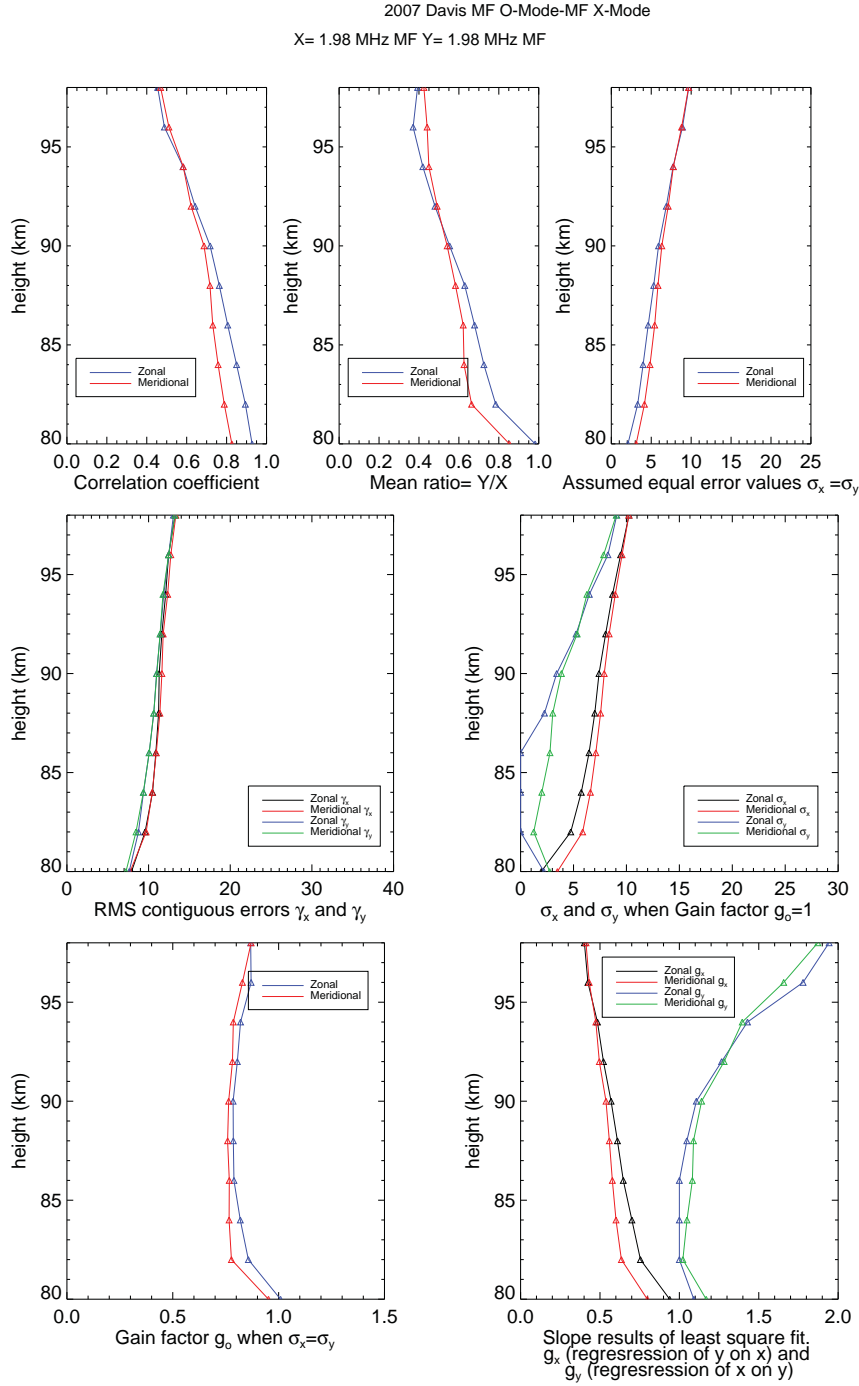


Figure C.7: Davis MF O-mode and X mode scatter plot comparison summary.

Appendix D

Supplementary Temperature Analysis Results

The following plots are supplementary results obtained during the course of analysing temperatures from different locations.

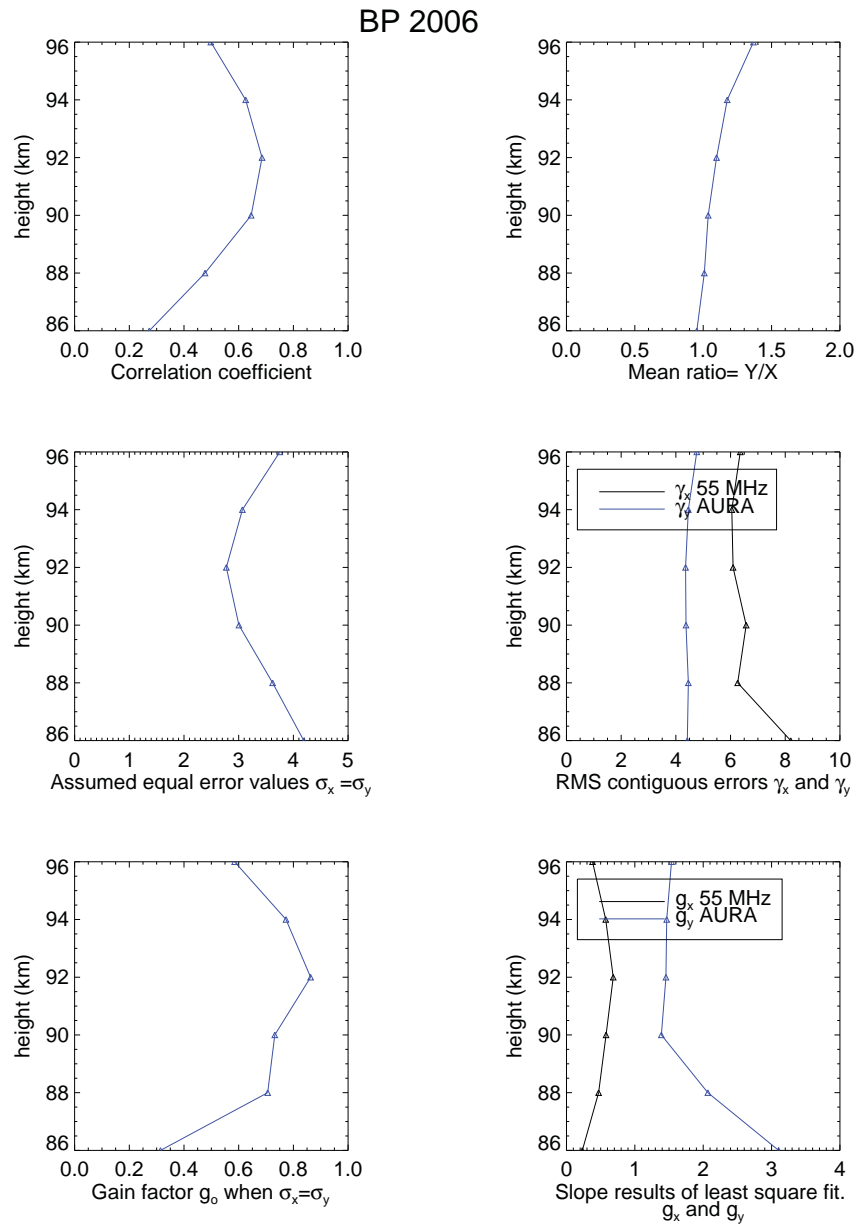


Figure D.1: 2006 BP 55 MHz Meteor radar and AURA MLS temperature comparison statistics.

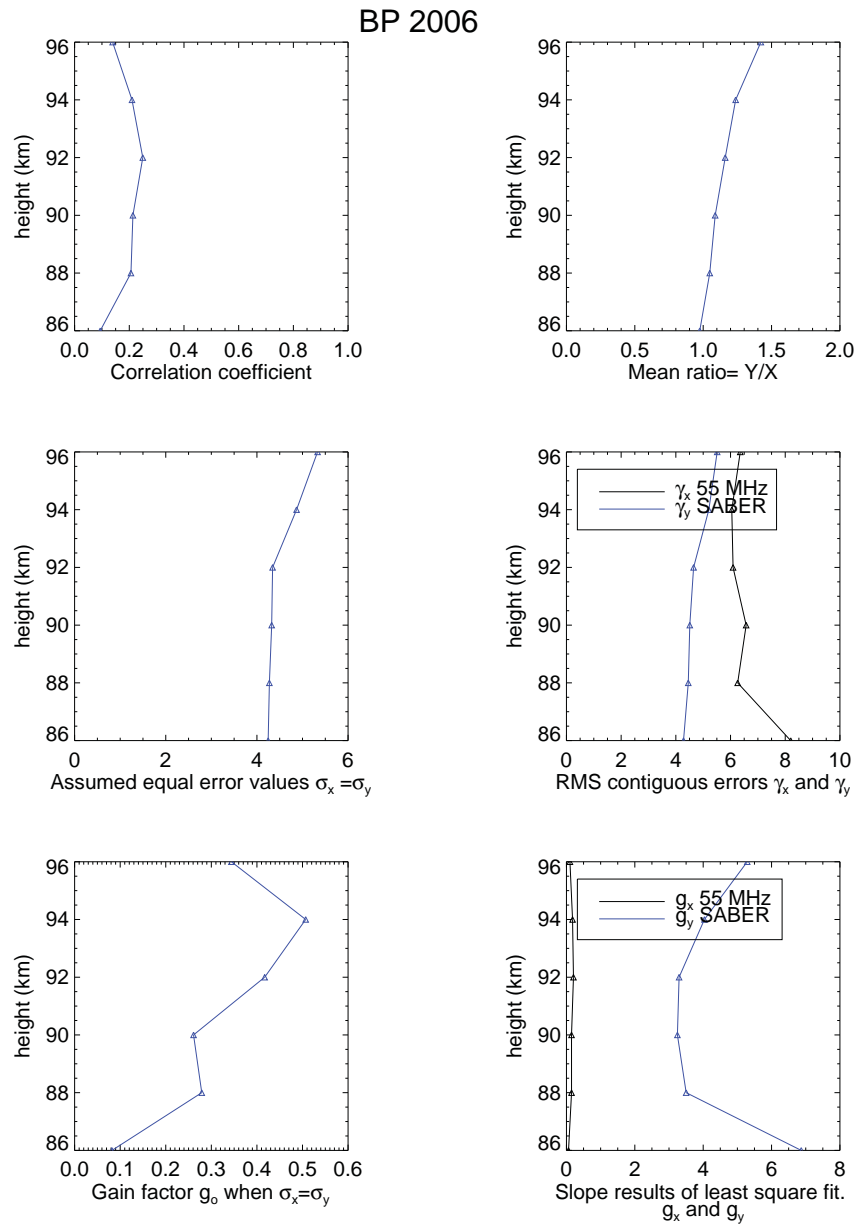


Figure D.2: 2006 BP 55 MHz Meteor radar and SABER temperature comparison statistics.

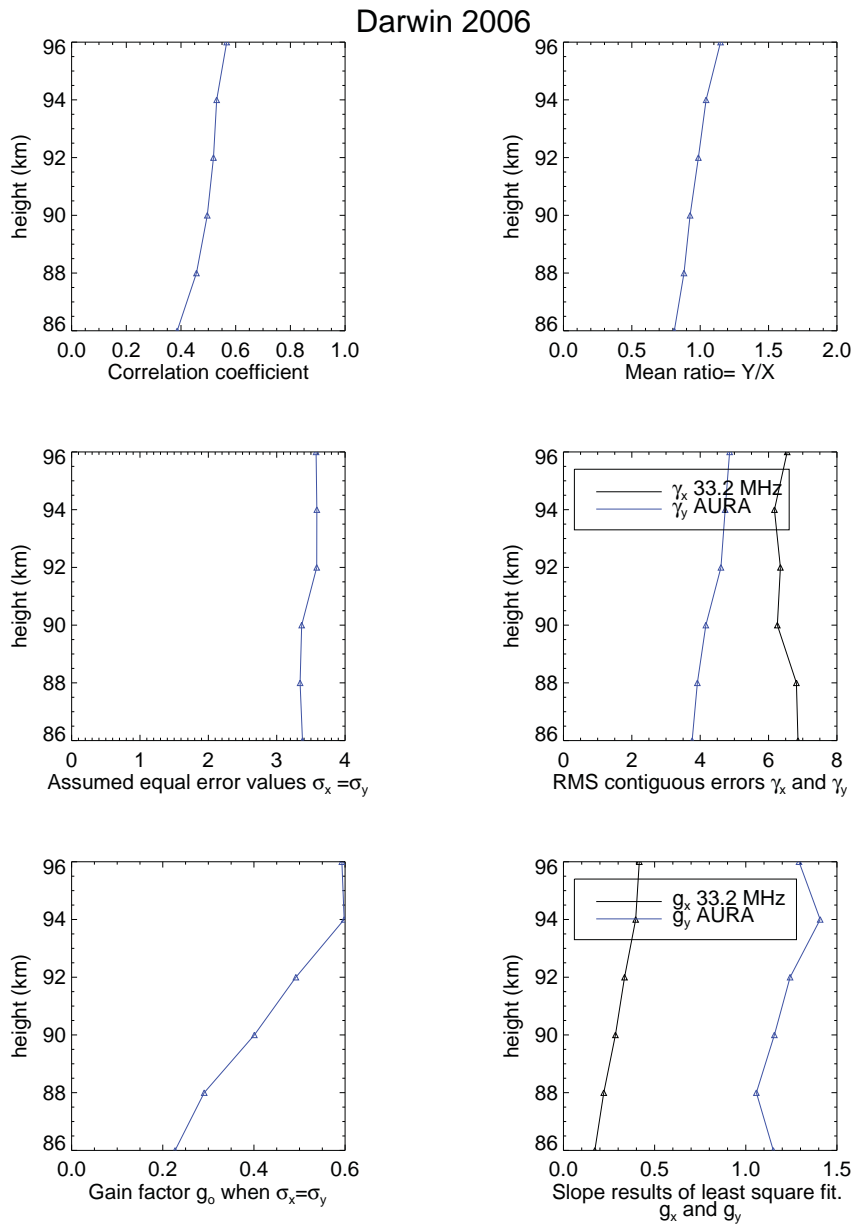


Figure D.3: 2006 Darwin 33.2 MHz Meteor radar and AURA MLS temperature comparison statistics.

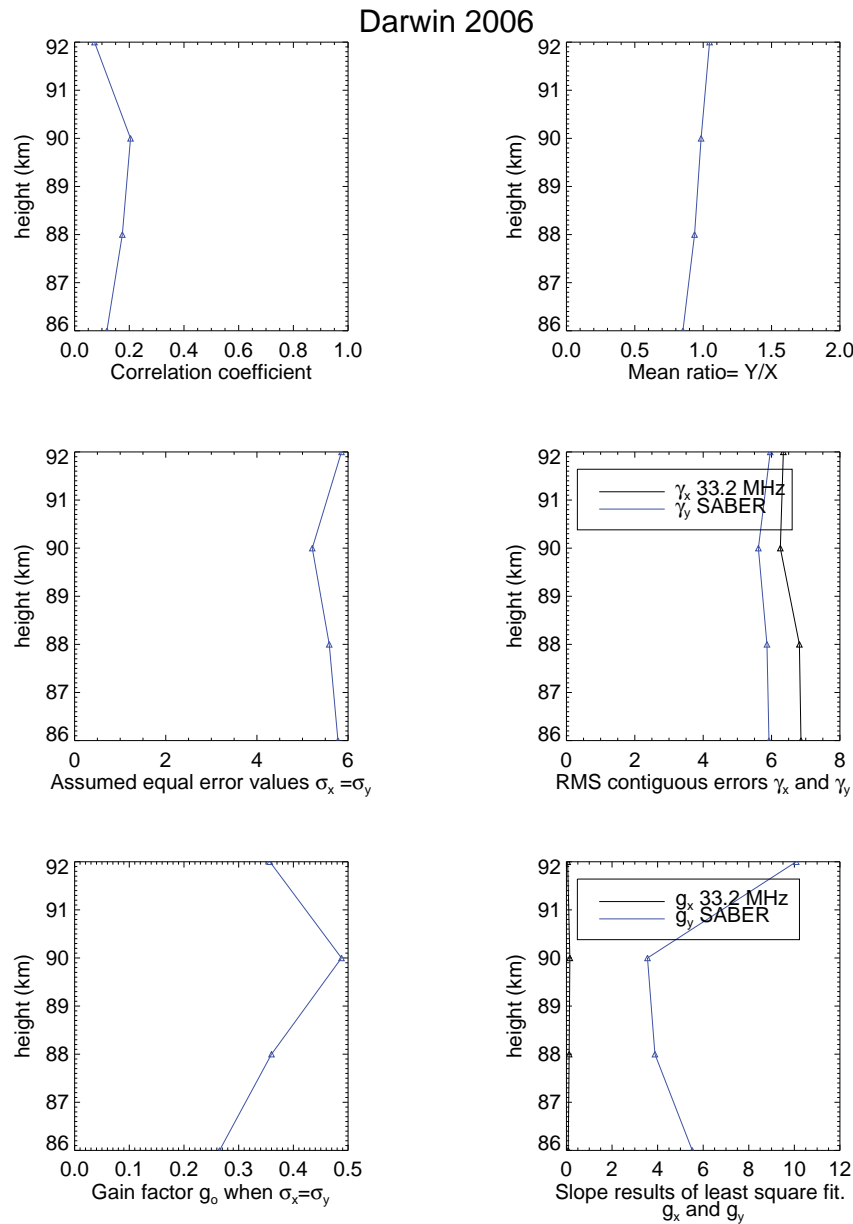


Figure D.4: 2006 Darwin 33.2 MHz Meteor radar and SABER temperature comparison statistics.

Bibliography

- W. J. Baggley and T. H. Webb. Measurements of the ionization heights of sporadic radio-meteors. *Mon. Not. R. Astron. Soc.*, 191:829–839, 1980.
- C. Balanis. *Antenna theory : analysis and design*. Wiley, 2nd edition, 1997.
- J. S. Belrose. Radio wave probing of the ionosphere by the partial reflection of radio waves (from heights below 100 km). *Journal of Atmospheric and Terrestrial Physics*, 32:567–596, April 1970.
- P. R Bevington and D. K Robinson. *Data reduction and error analysis for the physical sciences*. McGraw-Hill, second edition, 1992.
- B. Briggs and R. A. Vincent. Radar observation of atmospheric winds and turbulence: a comparison of techniques. *Journal of Atmospheric and Terrestrial Physics*, 42:823–833, 1980.
- B. H. Briggs. On the analysis of moving patterns in geophysics, -I. correlation analysis. *Journal of Atmospheric and Terrestrial Physics*, 30:1777–1788, 1968.
- G.B. Burns, W. J. R French, P. A. Greet, F. A. Phillips, P. F. B. Williams, K. Finlayson, and G. Klich. Seasonal variations and inter-year trends in seven years hydroxyl airglow rotational temperatures at davis station (69 degrees S, 78 degrees E), Antarctica. *Journal of Atmospheric and Solar-Terrestrial Physics*, 64:1167–1174, 2002.
- M. A. Cervera. *Meteor observations with a narrow beam VHF radar*. PhD thesis, University of Adelaide, Physics and Mathematical Physics, North Terrace, Adelaide, Febuary 1996.

- M. A Cervera and W. G Elford. The meteor radar response function: Theory and application to narrow beam MST radar. *planetary and space science*, 52:591–602, 2004.
- M. A. Cervera and I. M. Reid. Comparison of simultaneous wind measurements using colocated VHF meteor radar and MF spaced anatenna radar systems. *Radio Science*, 30:1245–1261, 1995.
- M. A Cervera and I. M. Reid. Comparison of atmospheric parameters derived from meteor observations with CIRA. *Radio Science*, 35, 3:833–843, 2000.
- M. A. Cervera, D. A. Holdsworth, and I. M. Reid. Meteor radar response function: Application to the interpretation of meteor backscatter at medium frequency. *Geophysical Research*, 109, 2004.
- C. Cevolani, M. F. Gabucci, G. Grassi, and G. Trivellone. Structural aspects of meteoroid streams observed by a forward scatter radar system. *planetary and space science*, 46(8):869–880, August 1998.
- P. Chilson, P. Czechowsky, and G. Schmidt. A comparison of ambipolar diffusion coefficients in meteor trains using VHF radar and UV lidar. *Geophysical Research Letters*, 23(20):2745–2748, 1996.
- Kenneth Davies. *Ionospheric Radio*. Number 31 in Electromagnetic Waves Series. Institution of Engineering and Technology, May 1990.
- L. P. Dyrud, M. M. Oppenheim, and A. F. vom Endt. The anomalous diffusion of meteor trails. *Geophysical Research Letters*, 28(14):2775–2778, July 2001.
- W. G Elford and D. S Robertson. Measurements of winds in the upper atmosphere by means of drifting meteor trails. *Journal of Atmospheric and Terrestrial Physics*, 4:271–284, 1953.
- W. G. Elford, Z. Ceplecha, J. Borovicka, D. O. Revelle, R. L. Hawkes, V. Porubcan, and M. Simek. Meteor phenomena and bodies. *Space Science Reviews*, 84:327–471, 1998.
- S. J. Franke, X. Chu, and A. Z. Liu. Comparison of meteor radar and Na doppler lidar measurements of winds in the mesopause region above Maui, Hawaii. *Journal of Geophysical Research*, 110(D09S02), January 2005.

- W. J. R French and G.B. Burns. The influence of large-scale oscillations on long-term trend assessment in hydroxyl temperatures over davis, antarctica. *Journal of Atmospheric and Solar-Terrestrial Physics*, 66:493–506, January 2004.
- W. J. R French, G.B. Burns, K. Finlayson, P. A. Greet, R. P. Lowe, and P. F. B. Williams. Hydroxyl (6-2) airglow emission intensity ratios for rotational temperature determination. *Annales Geophysicae*, 18:1293–1303, 2000.
- W. J. R French, G.B. Burns, and P. J. Espy. Anomalous winter hydroxyl temperatures at 69 degrees S during 2002 in a multilayer context. *Geophysical Research Letters*, 32(L12818), June 2005.
- L. Froidevaux, N. J. Livesey, W. G. Read, Y. B. B. Jiang, C. Jimenez, M. J. Filipiak, M. J. Schwartz, M. L. Santee, H. C. Pumphrey, J. H. Jiang, D. L. Wu, G. L. Manney, J. W. Drouin B. J., Waters, E. J. Fetzer, P. F. Bernath, C. D. Boone, K. A. Walker, K. W. Jucks, G. C. Toon, J. J. Margitan, B. Sen, C. R. Webster, L. E. Christensen, J. W. Elkins, E. Atlas, R. A. Lueb, and R. Hendershot. Early validation analyses of atmospheric profiles from EOS MLS on the Aura satellite. *IEEE Transactions on Geoscience and Remote Sensing*, 44:1106–1121, 2006.
- K. S. Gage and B. B. Balsley. On the scattering and reflection mechanisms contributing to clear air radar echoes from the troposphere, stratosphere, and mesophere. *Radio Science*, 15(2):243–257, 1980.
- F. F. Gardner and J. L. Pawsey. Study of the ionospheric d-region using partial reflections. *Journal of Atmospheric and Terrestrial Physics*, 3(6):321–324, July 1953.
- L. J. Gelinas, J. Hecht, R. L. Walterscheid, R. G. Roble, and J. M. Woithe. A seasonal study of mesospheric temperatures and emission intensities at adelaide and alice springs. *Journal of Geophysical Research*, 113:A01304, 2008.
- M. G. Golley and D. E. Rossiter. Some tests of methods of analysis of ionospheric drifts using an array of 89 aerials. *Journal of Atmospheric and Terrestrial Physics*, 32:1215–1233, 1970.

- M. Gracia-Comas, M. Lopez-Puertas, B. T. Marshall, P. P. Wintersteiner, B. Funke, D. Bermejo-Pantanleón, C. J. Mertens, E. E. Remsberg, L. L. Gordley, M. G. Mlynczak, and J. M. Russell III. Errors in sounding of the atmosphere using broadband emission radiometry (SABER) kinetic temperature caused by non-local-thermodynamic-equilibrium model parameters. *Journal of Geophysical Research*, 113(D24106), December 2008.
- H. E. Green. Design data for short and medium length Yagi-Uda arrays. *Electrical Engineering Transactions*, EE2, No.1:1–8, March 1966.
- C. M. Hall. On the influence of neutral turbulence on ambipolar diffusivities deduced from meteor trail expansion. *Annales Geophysicae*, 20(11):1857–1862, November 2002.
- C. M. Hall, T. Aso, M. Tsutsumi, J. Höffner, and F. Sigernes. Multi-instrument derivation of 90 km temperatures over Svalbard (78 degrees N, 16 degrees E). *Radio Science*, 39(6), November 2004.
- C. M. Hall, T. Aso, M. Tsutsumi, S. Nozawa, A. H. Manson, and C. E. Meek. A comparison of mesosphere and lower thermosphere neutral winds as determined by meteor and medium-frequency radar at 70 degrees N. *Radio Science*, 40(4), July 2005.
- C. M. Hall, T. Aso, J. Höffner, F. Sigernes, and D. A. Holdsworth. Neutral air temperatures at 90 km and 70 degrees N and 78 degrees N. *Journal of Geophysical Researchal of Geophysical*, 111(D14), July 2006.
- W. K Hocking and T. Thayaparan. Simultaneous and colocated observation of winds and tides by MF and meteor radars over london canada (43 degrees N, 81 degrees W), during 1994-1996. *Radio Science*, 32:833–865, 1997.
- W. K Hocking, J. Jones, and T. Thayaparan. Meteor decay times and their use in determining a diagnostic mesospheric temperature-pressure parameter: methodology and one year of data. *Geophysical Research Letters*, 24: 2977–2980, 1997.
- W. K Hocking, T. Thayaparan, and S. J. Franke. Method for statistical comparison of geophysical data by multiple instruments which have differing accuracies. *Adv. Space Res*, 27:1089–1098, 2001.

- W. K. Hocking, W. Singer, J. Bremer, N.J. Mitchell, P. Batista, B. Clemesha, and M. Donner. Meteor radar temperatures at multiple sites derived with SKiYMET radars and compared to OH, rocket and lidar measurements. *Journal of Atmospheric and Solar-Terrestrial Physics*, 66:585–593, 2004.
- D. A. Holdsworth and I. M. Reid. A simple model of atmospheric backscatter: Description and application to the full correlation analysis of spaced antenna data. *Radio Science*, 30(4), August 1995.
- D. A. Holdsworth and I. M. Reid. Comparisons of Full Correlation Analysis (FCA) and Imaging Doppler Interferometry (IDI) winds using the Buckland Park MF radar. *Annales Geophysicae*, 22(11):3829–3842, 2004a.
- D. A. Holdsworth and I. M. Reid. The Buckland Park MF radar: routine observation scheme and velocity comparisons. *Annales Geophysicae*, 22(11):3815–3828, November 2004b.
- D. A. Holdsworth, I. M. Reid, and M. A. Cervera. Buckland Park all-sky interferometric radar. *Radio Science*, 39, 2004.
- D. A. Holdsworth, R. J. Morris, D. J. Murphy, I. M. Reid, G.B. Burns, and W. J. R French. Antarctic mesospheric temperature estimation using the Davis mesospheric-startospheric-tropospheric radar. *Journal of Geophysical Research*, 111, 2006.
- G. O. L. Jones, F. T. Berkey, C. S. Fish, W. K Hocking, and M. J. Taylor. Validation of Imaging Doppler Interferometer winds using meteor radar. *Geophysical Research Letters*, 30(14):1743, July 2003.
- J. Jones, A. R. Webster, and W. K. Hocking. An improved interferometer design for use with meteor radars. *Radio Science*, 33:55–65, 1998.
- W. Jones. Theory of diffusion of meteor trains in the geomagnetic field. *Planetary Space Science*, 39 No. 9:1283–1288, 1991.
- W. Jones. Theory if the initial radius of meteor trains. *Monthly Notices of the Royal Astronomical Society*, 275:812–818, 1995.
- W. Jones and J. Jones. Ionic diffusion in meteor trains. *Atmospheric and Terrestrial Physics*, 52 No. 3:185–191, 1990.

- K. K. Kumar, G. Ramkumar, and S. T. Shelbi. Initial results from SKiMET meteor radar at Thumba (8.5 degrees N, 77 degrees E):1. comparison of wind measurements with MF spaced antenna radar system. *Radio Science*, 42:RS6008, December 2007.
- K. K. Kumar, C. Vineeth, T. M. Antonita, T. K. Pant, and R. Sridharan. Determination of day-time OH emission heights using simultaneous meteor radar, day-glow photometer and TIMED/SABER observations over Thumba (8.5 degrees N, 77 degrees E). *Geophysical Research Letters*, 35 (L18809), September 2008.
- S. R. Langhoff, J Werner, H, and R Rosmus. Theoretical transition probabilities for the OH Meinel system. *Journal of Molecular Spectroscopy*, 118: 507–529, 1986.
- F. J. Lübken. Thermal structure of the arctic summer mesosphere. *Journal of Geophysical Research*, 27:9135–9149, 1999.
- F. J. Lübken and U. von Zahn. Thermal structure of the mesopause region at polar latitudes. *Journal of Geophysical Research*, 20:20,841–20,857, 1991.
- F. J. Lübken, A. Müllemann, and M. J. Jarvis. Temperatures and horizontal winds in the Antarctic summer mesosphere. *Journal of Geophysical Research*, 109(D24112), 2004.
- A. MacKinnon. *VHF Boundary Layer Radar and RASS*. PhD thesis, University of Adelaide, 2001.
- E. A. Mason and E. W. McDaniel. *Transport properties of Ions in Gases*. John Wiley, 1988.
- H. S. W. Massey. *Electronic and Ionic impact Phenomena*, volume 3. Oxford at the Clarendon press, second edition, 1971.
- J. D. Matthews. Radio science issues surrounding HF/VHF/UHF radar meteor studies. *Journal of Atmospheric and Solar-Terrestrial Physics*, 66(6-4): 285–299, 2004.
- P. T. May and J. H. Mather. Experiment to characterize tropical cloud systems. *EOS*, 86(31):2, August 2005.

- H. G. Mayr, J. G. Mengel, C. O. Hines, K. L. Chan, N. F. Arnold, C. A. Reddy, and H. S. Porter. The gravity wave Doppler spread theory applied in numerical spectral model of the middle atmosphere .1. Model and global scale seasonal variations. *Journal of Geophysical Research-Atmospheres*, 102(D22):26077–26091, November 1997.
- H. G. Mayr, J. G. Mengel, and F. T. Huang. Modelling the temperature of the polar mesopause region: Part i - Inter-annual and long-term variations generated by the stratospheric QBO. *Journal of Atmospheric and Solar-Terrestrial Physics*, 71(3-4):497–507, March 2009.
- D. W. R. McKinley. Variation of meteor echo rates with radar system paramters. *Canadian Journal of Physics*, 29:403–426, 1951.
- D. W. R. McKinley. *Meteor Science And Engineering*. Number 523.5 M15 in Engineering Sciences. McGraw-Hill, first edition, 1961.
- H. Nagaoka. Possibility of disturbance of radio transmissions by meteoroic showers. *Proceedings of the Imperial Academy of Tokyo*, 5(233), 1929.
- F. I. Peregudov. On the effect of meteor velocities on the hour number in radio-echo detection of meteors. *Soviet Astr.*, 2:833–388, 1958.
- F. Phillips, G.B. Burns, W. J. R French, P. F. B. Williams, A. R. Klekociuk, and R. P. Lowe. Determining rotational temperatures from the OH(8-2) band, and a comparison with OH(6-2) rotational temperatures at Davis, Antarctica. *Annales Geophysicae*, 22:1549–1561, April 2004.
- J. A. Ratcliffe. *The Magneto-Ionic Theory and its Applications to the Ionosphere*. Cambridge University Press, 1962.
- J. A. Ratcliffe. The Early Ionosphere Investigations of Appleton and His Colleagues. *Philosophical Transactions for the Royal Society of London*, 280(1293):3–9, October 1975.
- I. M. Reid. Radar observations of stratified layers in the mesosphere and lower thermosphere (50-100 km). *Advances in Space Research*, 10(10), 1990.
- I. M. Reid and J. M. Woithe. Three-field photometer observations of short-period gravity wave intrinsic paramters in the 80 to 100 km height region. *Journal of Geophysical Research*, 110(D21), November 2005.

- I. M. Reid, B. G. W. Vanderpeer, S. C. Dillon, and B. M. Fuller. The new Adelaide medium frequency Doppler radar. *Radio Science*, 30(4):1177–1189, 1995.
- H. Rishbeth and O. K. Garriot. *Introduction to ionospheric physics*, volume 14 of *International geophysics series*. Academic Press, 1969.
- R.G. Roper. *Some Mesopause Level Dynamics*. DSc Thesis, University of Adelaide, 3 edition, August 2008.
- M. J. Schwartz, A. Lambert, G. L. Manney, W. G. Read, N. J. Livesey, L. Froidevaux, C. O. Ao, P. F. Bernath, C. D. Boone, R. E. Cofield, W. H. Daffer, Drouin B. J., E. J. Fetzer, R. A. Fuller, R. F. Jarnot, J. H. Jiang, Y. B. B. Jiang, B. W. Knosp, K. Krüger, J. L. F. Li, M. G. Mlynczak, S. Pawson, J. M. Russell III, M. L. Santee, W. V. Snyder, P. C. Stek, R. P. Thurstans, A. M. Tompkins, P. A. Wagner, K. A. Walker, J. W. Waters, and D. L. Wu. Validation of the AURA Microwave Limb Sounder temperature and geopotential height measurements. *Journal of Geophysical Research*, 113(D15), May 2008.
- M. G. Shepherd, W. F. J. Evans, G. Hernandez, D. Offermann, and H. Takahashi. Global variability of mesospheric temperature: Mean temperature field. *Journal of Geophysical Research*, 109(D24117), December 2004.
- W. Singer, R. Latteck, and D. A. Holdsworth. A narrow beam doppler radar at 3 MHz for studies of high-latitude middle atmosphere. *Adv. Space Res*, 41:1487–1493, 2008.
- A. M. Skellett. The Effect of Meteors on Radio Transmission Through the Kennelly-Heaviside Layer. *Physical Review Letters*, 37(12), June 1931.
- D. I. Steel and W. G. Elford. The height distribution of radio meteors: comparison of observations at different frequencies on the basis of standard echo theory. *Journal of Atmospheric and Terrestrial Science*, 53:409–417, 1991.
- J. R Taylor. *An Introduction to Error Analysis*. Mill Valley, 1982.
- M. Tsutsumi and T. Aso. Mf radar observations of meteors and meteor-derived winds at Syowa (69 degrees S, 39 degrees E), Antarctica: A com-

- parson with simultaneous spaced antenna winds. *Journal of Geophysical Research*, 110, 2005.
- M. Tsutsumi, A. S. Yukimatu, D. A. Holdsworth, and M. Lester. Advanced SuperDARN meteor wind observations based on raw time series analysis technique. *Radio Science*, 44, March 2009.
- M. Tsutsumi, M., T. Tsuda, and T. Nakamura. Temperature fluctuations near the mesopause inferred from meteor observations with the middle and upper atmosphere radar. *Radio Science*, 29:599–610, 1994.
- P. F. B. Williams. OH rotational temperatures at Davis, Antarctica, via scanning spectrometer. *Planetary Space Science*, 44:163–170, 1996.
- J. Xu, C. Y. She, W. Yuan, C. J. Mertens, M. Mlynczak, and J. Russell. Comparison between the temperature measurements by TIMED/SABER and lidar in the midlatitude. *Journal of Geophysical Research*, 111(A10S09), 2006.
- J. Younger, I. M. Reid, R. A. Vincent, and D. A. Holdsworth. Modelling and observing the effect of aerosols on meteor radar measurements of the atmosphere. *Geophysical Research Letters*, 35:L15812, 2008.